# Pressure Perturbation Calorimetric Studies on Phospholipid-Sterol Mixtures

Linus Okoro and Roland Winter

Dortmund University of Technology, Faculty of Chemistry, Physical Chemistry I – Biophysical Chemistry, Otto-Hahn-Straße 6, D-44227 Dortmund, Germany

Reprint requests to Prof. Dr. R. Winter. Fax: +49-231-755-3901.
E-mail: roland.winter@tu-dortmund.de

*Z. Naturforsch.* **2008**, *63b,* 769 – 778; received February 18, 2008

*Dedicated to Professor Gérard Demazeau on the occasion of his 65$^{th}$ birthday*

Sterols regulate biological processes and sustain the lateral structure of cellular membranes. The sterol cholesterol, its precursor lanosterol, the plant sterols stigmasterol and ergosterol as well as 7-dehydrocholesterol were added up to 36 mol-% to vesicles of the phospholipid 1,2-dipalmitoyl-*sn*-glycero-3-phosphatidylcholine (DPPC). The aim of this study was to investigate the influence of the sterol side chain and ring structure on the volumetric properties of the lipid bilayer system by using pressure perturbation calorimetry (PPC), a relatively new and efficient technique, to study the thermal expansion coefficient and volumetric properties of biomolecules. The experiments were carried out in the temperature range from 10 to 85 °C, *i. e*., at temperatures below and above the chain-melting transition temperatures of the lipid mixtures. Additionally, corresponding differential scanning calorimetric (DSC) measurements were carried out. Whereas the conformational properties of the different sterols have a significant effect on the order parameter of the lipid acyl-chains, the thermodynamic parameters of these sterols are less influenced by the differential structural changes of the sterols. For lanosterol and stigmasterol, marked differences are found, however.

*Key words:* Pressure Perturbation Calorimetry, Coefficient of Thermal Expansion, Volume Change, Phospholipids, Sterols

## Introduction

Sterols, such as cholesterol, are important for the structural, dynamical as well as functional properties of biological membranes [1 – 4]. They are found in high concentrations (even up to about 50 mol-%) in plasma membranes of animal and higher plant cells, but in markedly lower concentrations in intracellular membranes where they are synthesized. A considerable amount of research has been devoted to elucidate the different biological functions of sterols and to understand the physical basis for their evolution by investigating the role of sterols in modulating physical properties of artificial and biological membranes, and to unravel the relationship between their function and molecular structure [1 – 7].

Cholesterol (see Fig. 1) has a hydrophobic and planar fused tetracyclic ring structure with two $\beta$-oriented methyl groups at positions 10 and 13, a branched extended iso-octyl side chain at position C17, and a hydrophilic $\beta$-oriented hydroxyl group at position C3. The sterol ring orients itself parallel with the acyl-chains of the membrane phospholipids, with its 3 $\beta$-OH group in proximity to the phospholipid ester carbonyl oxygen at the lipid–water interface. Van der Waals interactions between the lipid acyl-chains and the sterol ring as well as its branched side chain seem to be the most important contributions stabilizing cholesterol-phospholipid interactions. It has been demonstrated by a variety of physical techniques [7] that cholesterol has a "condensing" (ordering) effect on the packing of phospholipids in their fluid-like (liquid-crystalline) state, because the rigid ring structure of the sterol limits the possibility for *cis-trans* isomerizations and kink formation of neighboring lipid chains, and a disordering effect below the chain-melting transition, *i. e*., in the gel state of the lipid bilayer. The extent of these effects depends on the detailed molecular structure of the lipid, but probably also on the sterol conformation and stereochemistry [5 – 30]. Whereas structural and dynamical properties of these systems have been studied to a significant extent, there is a

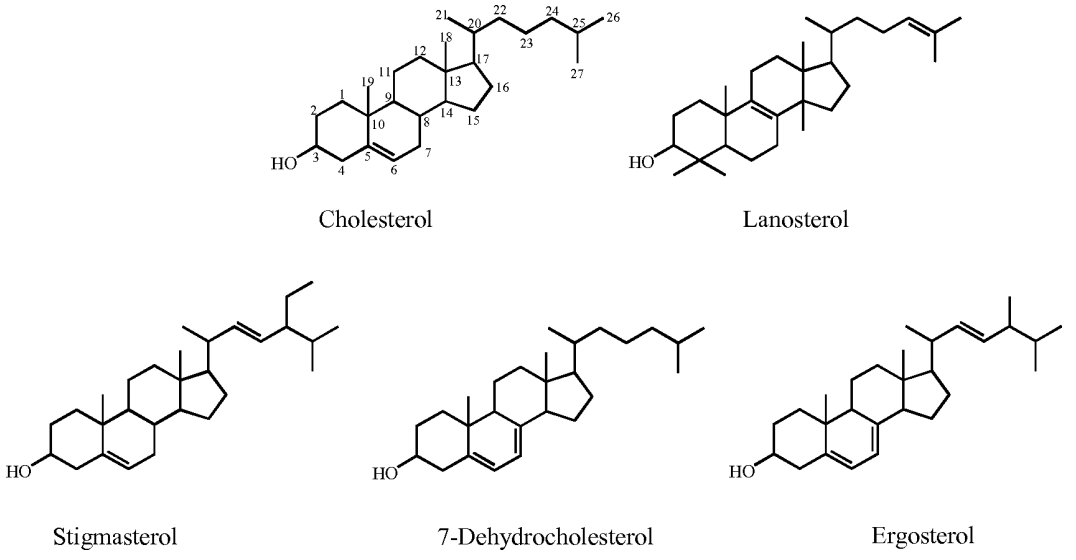


Fig. 1. The chemical structures of the sterols used in this study. The formula of cholesterol includes the numbering of the carbon atoms.

lack of knowledge of thermodynamic functions of these systems [31 – 34]. In this study, we investigated volumetric properties of lipid vesicles of the common phospholipid 1,2-dipalmitoyl-*sn*-glycero-3-phosphatidylcholine (DPPC), containing different amounts of various sterols up to 36 mol-% sterol.

DPPC phospholipid bilayers exhibit two principal thermotropic lamellar phase transitions, corresponding to a gel-to-gel ($L_{\beta'}$-$P_{\beta'}$) pretransition and a gel-to-liquid-crystalline ($P_{\beta'}$-$L_{\alpha}$) main transition at $T_m \approx$ 41.5 °C [35]. In the fluid-like $L_{\alpha}$ phase, the hydrocarbon chains of the lipid bilayer are conformationally disordered, whereas in the gel phases, the hydrocarbon chains are more extended and relatively ordered. In general, sterol molecules are, in contrast to phospholipids, essentially rigid and relatively smooth in their hydrophobic parts. They prefer to have next to them lipid acyl-chains that are ordered. On the other hand, because the sterols have different molecular shapes owing to conformationally ordered lipid chains, they tend to break the lateral packing of solid-ordered ($s_o$) phases. This can lead to the emergence of a physical state of lipid-sterol membranes, which has characteristics intermediate between solid-ordered and liquid-disordered ($l_d$), *viz.* the liquid-ordered ($l_o$) state. In recent years, cholesterol-rich liquid-ordered ($l_o$) structures have received much attention in membrane biophysics. A hypothesis has been put forward that so-called rafts, which are liquid-ordered domain structures enriched in cholesterol and sphingolipids, exist in cell membranes and have potential functional importance in processes such as intracellular membrane sorting and signal transduction at the cell surface [36]. Only for selected phospholipid-sterol systems, temperature-concentration phase diagrams are available [7, 20 – 26]. They exhibit the one-phase regions $l_d$ (liquid-disordered), $s_o$ (solid-ordered), and $l_o$ (liquid-ordered). In addition, $l_o$+$s_o$ and $l_o$+$l_d$ two-phase coexistence regions – separated by a three-phase line – are found in the intermediate sterol concentration range at low and high temperatures, respectively. (The terms 'solid' and 'liquid' characterize mainly the fluidity of a phase, whereas 'ordered' and 'disordered' indicate the conformational state (order parameter) of the lipid acyl-chains.) At sufficiently high temperatures, the $l_o$+$l_d$ two-phase regions seem to be terminated in a critical point.

The focus of our study was to identify and characterize the differential effects of various sterols (Fig. 1) including cholesterol, ergosterol (which is essential in some fungi or protozoan cells), the plant sterol stigmasterol, *trans*-7-dehydrocholesterol (7-DHC), and lanosterol, the evolutionary precursor of cholesterol, on equilibrium volumetric properties of the DPPC bilayer membrane and to relate these effects to the difference in their molecular structure. To this end, pressure perturbation calorimetry (PPC) has been used, which allows determination of the temperature depen-

dence of the coefficient of expansion, $\alpha$, as well as volume changes accompanying lipid phase transitions. The PPC measurements were carried out over a wide temperature range in order to cover all relevant phase regions of these DPPC-sterol mixtures. Complementary DSC thermograms were also recorded to reveal temperature-dependent phase changes.

## Materials and Methods

1,2-Dipalmitoyl-*sn*-glycero-3-phosphocholine (DPPC) was obtained from Avanti Polar Lipids (Alabaster, AL). Cholesterol, 7-dehydrocholesterol (7-DHC), lanosterol, and stigmasterol were obtained from Sigma-Aldrich (St. Louis, MO), while ergosterol was obtained from Fluka, Germany. All sterols were purchased as dry powders and used without further purification. Multilamellar vesicles (MLV) of DPPC and sterol with designated mole ratios were mixed in chloroform and dried as a thin film under a stream of nitrogen and then freeze-dried overnight. The lipid films were hydrated in a Tris-HCl buffer (10 mM Tris-HCl, 100 mM NaCl, pH = 7.4), followed by vortexing and five freeze-thaw cycles.

Pressure perturbation calorimetry and differential calorimetry measurements were performed with a MicroCal (Northampton, USA) VP-DSC micro-calorimeter, equipped with a pressurizing system from the same manufacturer. The reference cell was filled with the Tris-HCl buffer solution. Both buffer and lipid/sterol solutions were degassed before being injected into the respective cells. Included in the standard VP-DSC instrument is a pressuring cap that allows application of 1.8 bar to the cells in order to avoid air bubbles at elevated temperatures. The instrument was operated in the high-gain mode at a scanning rate of 40 °C $h^{-1}$. Baseline subtraction (pure buffer) and normalization with respect to scan rate and concentration were performed by the instrument software, yielding the temperature-dependent apparent (excess) molar heat capacity of the lipid/sterol vesicles, $C_p$, with respect to the buffer solution. The sample concentration of the lipid in buffer was 20 mg $mL^{-1}$.

Pressure perturbation calorimetry (PPC) measurements were carried out on the VP-DSC calorimeter equipped with MicroCal's (Northampton, MA, USA) PPC accessory. A description of the technique and its potential applications has been placed elsewhere [37–43]. This still rather novel method allows to measure heat effects induced by small periodic changes of gas pressure ($\Delta p = \pm 5$ bar) above the solution. The physical principle is the same as in a heat-induced thermal expansion, although the measurable is $\Delta Q$, the heat released upon a pressure change of $\Delta p$ at temperature $T$. Knowing the thermal expansion coefficient of the solvent, $\alpha_0$, the mass, $m$, and the partial specific volume of the solute, $V$, through a series of reference measurements, one can calculate the apparent thermal expansion coefficient of the dissolved particles:

$$\alpha = \alpha_0 - \frac{\Delta Q}{T \Delta p m V} \tag{1}$$

The relative volume change $\Delta V/V$ at a phase transition, taking place in the temperature range from $T_o$ to $T_e$, can be obtained by integration of $\alpha(T)$:

$$\frac{\Delta V}{V} = \int_{T_o}^{T_e} \alpha(T) \mathrm{d}T \tag{2}$$

Three control and calibration measurements were performed, namely water (sample cell) *versus* water (reference cell), buffer *versus* water and buffer *versus* buffer. The results of these control experiments were fit by second-order polynomials and were used for the evaluation of the coefficient of thermal expansion $\alpha(T)$ of the lipid/sterol system. From the relative volume changes $\Delta V/V$, the absolute volume changes $\Delta V$ can be determined when the specific volume and the molar mass of the sample is known [30, 32, 44].

## Results and Discussion

For all lipid mixtures studied, DSC and PPC scans have been measured for a series of sterol concentrations, ranging from 5 to 36 mol-%. Fig. 2a shows the DSC scans (as stacked plot) of DPPC dispersions containing different concentrations of cholesterol. Pure DPPC displays a sharp transition at the main gel-to-fluid transition at $T_m$ = 41.5 °C, and a small endothermic peak due to the $L_{\beta'}$-$P_{\beta'}$ pretransition which appears around 35 °C. For 5 mol-% cholesterol, the transitions broaden and shift towards lower temperatures. The transition enthalpies $\Delta H$ decrease concomitantly. As the cholesterol concentration increases to 12 mol-% and higher, the main transition peak intensity decreases and broadens drastically, producing a multicomponent DSC endotherm consisting of a sharp component (arising from the fairly cooperative melting of domains enriched on DPPC) that is progressively reduced in

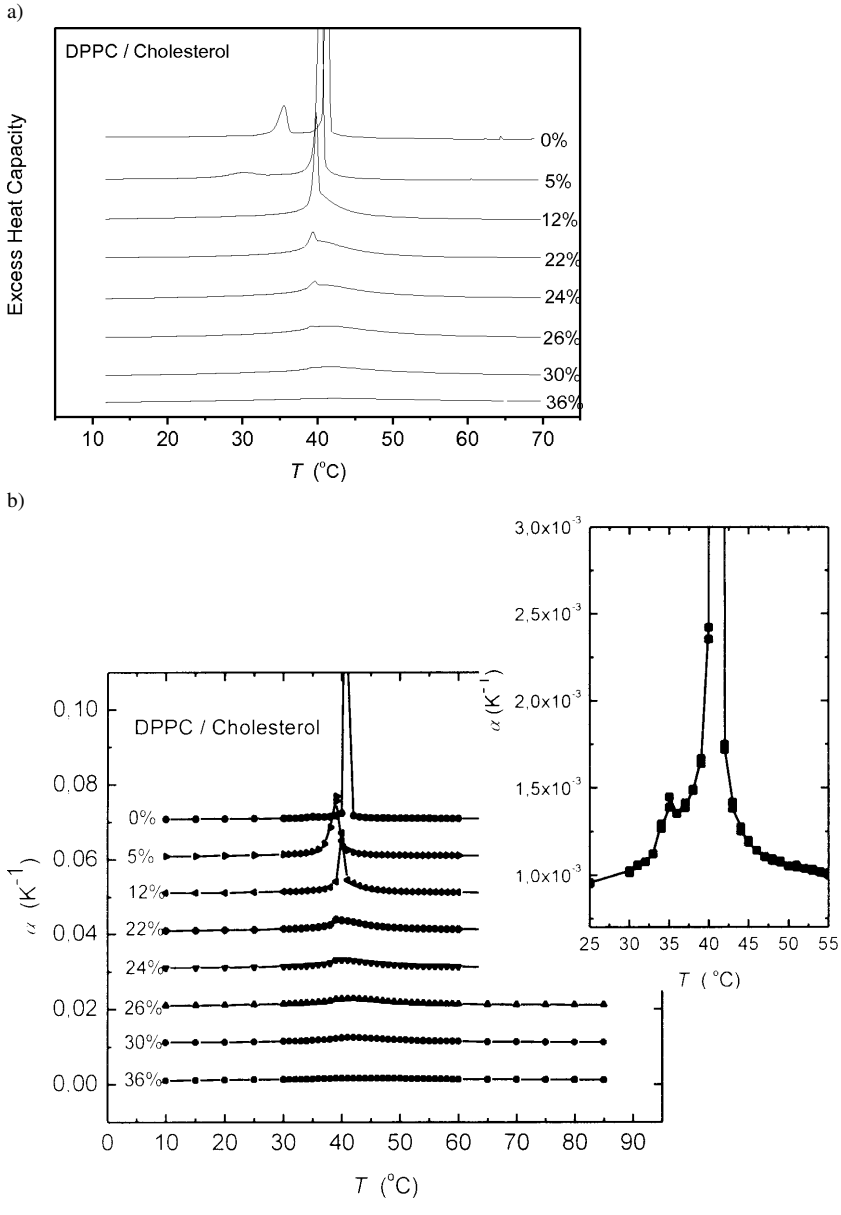


Fig. 2. a) DSC thermograms (heating scans only) of pure DPPC and DPPC/cholesterol mixtures in excess water. The thermograms were acquired at the sterol concentrations (in mol-%) indicated and have all been normalized against the mass of DPPC used. b) Temperature dependence of the coefficient of thermal expansion, $\alpha$, of pure DPPC and DPPC/cholesterol mixtures (pH = 7.4, 10 mM Tris buffer, scan rate 40 °C $h^{-1}$). For better visibility, the curves are displaced along the $y$ axis (from bottom to top by 0.01 units). For the data of pure DPPC, an expanded scale is given on the right-hand side.

temperature, enthalpy and cooperativity (width), and a broad component that increases in both temperature and enthalpy, but decreases in cooperativity, in agreement with literature data [27 – 29]. The DSC thermogram can be interpreted in terms of a transition from a $s_o$+$l_o$ two-phase region to an all-fluid $l_d$ phase at high temperatures (above ∼55 °C), thereby passing through a $l_o$+$l_d$ two-phase region above about 40 °C [23, 24, 27, 29]. Whereas at 30 mol-% cholesterol a weak and broad DSC endotherm is still observed, at 36 mol-% cholesterol, no phase transitions seem to be visible anymore.

Fig. 3a shows the DSC data for DPPC/ergosterol. In agreement with data from Hsueh *et al*. [23], at 5 mol-% ergosterol, the main transition becomes broadened and shifts toward lower temperature, indicating a $s_o$ and $l_d$ phase coexistence region. As the ergosterol concentration increases to 22 mol-%, the intensity of the main DSC peak decreases, and the peak position seems to remain essentially unchanged. A broad shoulder appears

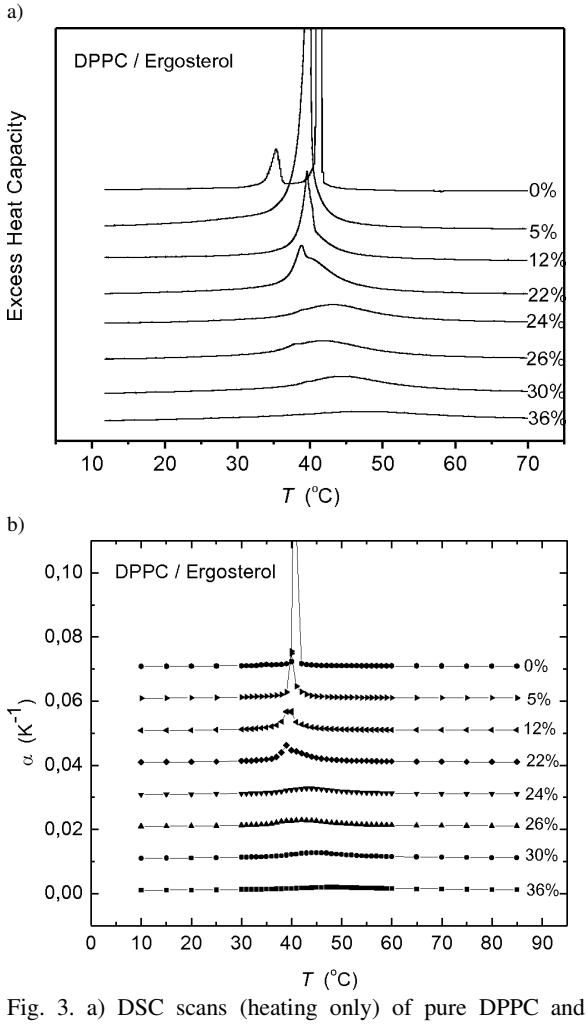


Fig. 3. a) DSC scans (heating only) of pure DPPC and DPPC/ergosterol mixtures in excess water. b) Temperature dependence of the coefficient of thermal expansion, $\alpha$, of pure DPPC and DPPC/ergosterol mixtures (pH = 7.4, 10 mM Tris buffer, scan rate 40 °C $h^{-1}$).

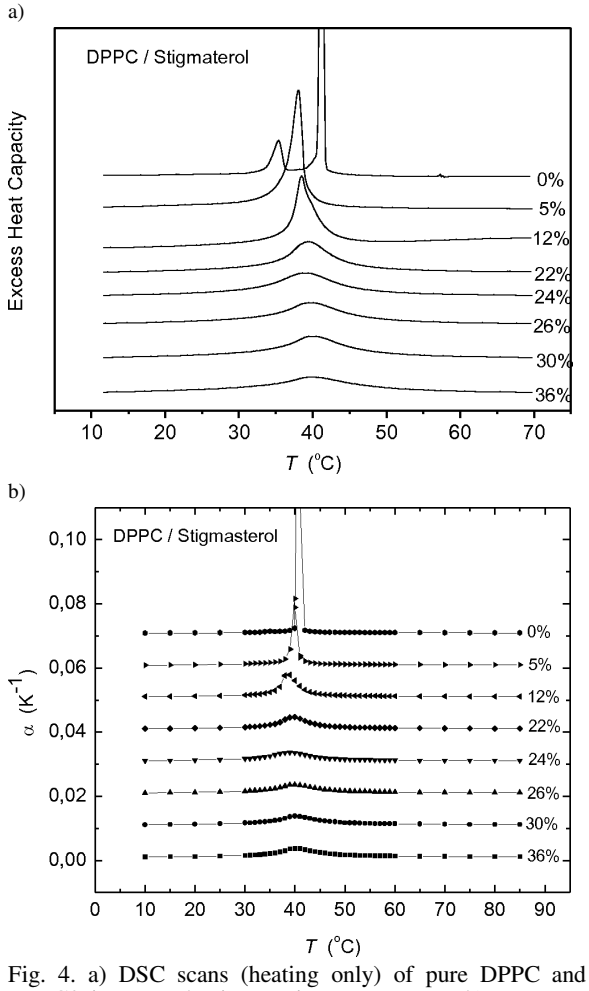


Fig. 4. a) DSC scans (heating only) of pure DPPC and DPPC/stigmasterol mixtures in excess water. b) Temperature dependence of the coefficient of thermal expansion, $\alpha$, of pure DPPC and DPPC/stigmasterol mixtures (pH = 7.4, 10 mM Tris buffer, scan rate 40 °C $h^{-1}$).

on the high-temperature side of the sharp peak, also suggesting a $l_d$+$l_o$ two-phase region. Where the broad peak ends, the transition to the $l_d$ phase occurs. At ergosterol concentrations of 30 mol-% and above, a very broad residual endotherm is observed only, similar to that seen in DPPC-cholesterol MLV.

The DSC thermograms of the systems DPPC/stigmasterol and DPPC/7-DHC exhibit a similar concentration dependence (Figs. 4a, 5a). For stigmasterol, no sharp component is observed in the DSC thermograms above 12 mol-% sterol, rather a broad DSC peak centered around 40 – 41 °C, only. However, there are significant differences in the pattern of thermal events observed for the system DPPC/lanosterol (Fig. 6a) at concentrations above 12 mol-%, indicating that the phase behavior of this system is qualitatively different at high sterol concentrations. No pronounced $l_d$+$l_o$ phase coexistence region above $T_m$ is discernible (see also [7, 29]). Also for 5 mol-% lanosterol, no pretransitional peak is observed, indicating that lanosterol is more effective at abolishing the pretransition than cholesterol on a molar basis, in agreement with literature data [7, 29].

Generally, the thermodynamic variables $C_p$ and $\alpha$ are directly related to fluctuation parameters. The square average of the enthalpy fluctuations, $\langle \Delta H^2 \rangle$, is determined by the heat capacity, $C_p$, of the system, and

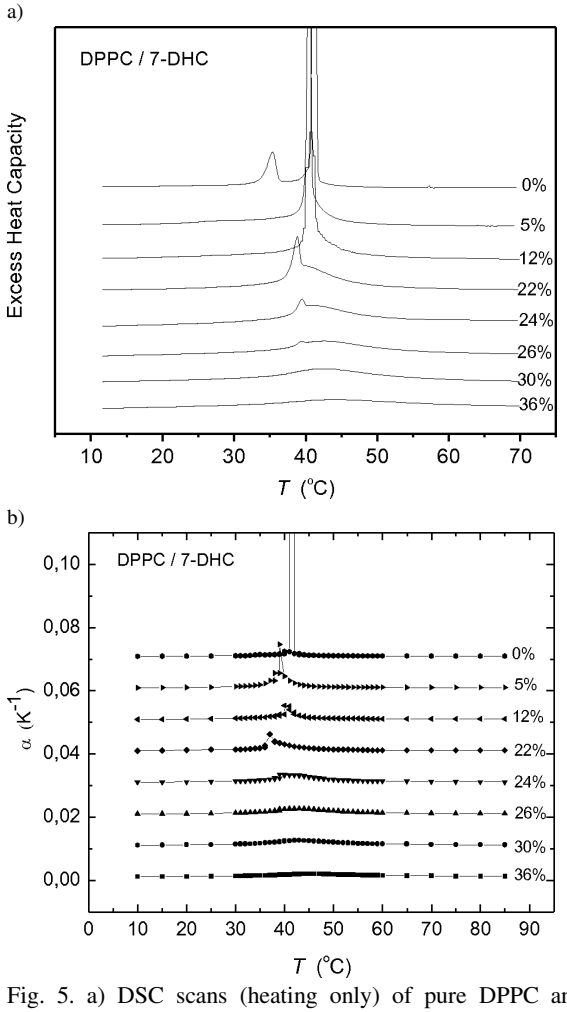


Fig. 5. a) DSC scans (heating only) of pure DPPC and DPPC/7-dehydrocholesterol (7-DHC) mixtures in excess water. b) Temperature dependence of the coefficient of thermal expansion, $\alpha$, of pure DPPC and DPPC/7-dehydrocholesterol (7-DHC) mixtures (pH = 7.4, 10 mM Tris buffer, scan rate 40 °C h$^{-1}$).

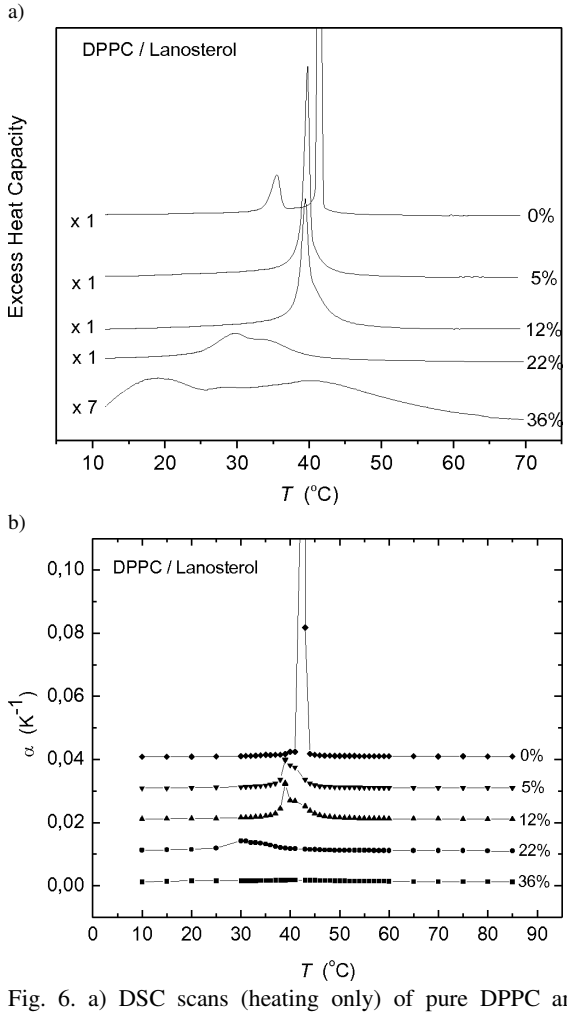


Fig. 6. a) DSC scans (heating only) of pure DPPC and DPPC/lanosterol mixtures in excess water. b) Temperature dependence of the coefficient of thermal expansion, $\alpha$, of pure DPPC and DPPC/lanosterol mixtures (pH = 7.4, 10 mM Tris buffer, scan rate 40 °C h$^{-1}$); $y$ axis scaling factors were used as indicated on the left-hand side of the thermogram.

the covariance between $H$ and $V$ fluctuations, $\langle \Delta H \Delta V \rangle$, is related to the thermal expansion [45]:

$$\langle \Delta H^2 \rangle = RT^2 C_p, \tag{3}$$

$$\langle \Delta H \Delta V \rangle = RT^2 V \alpha. \tag{4}$$

Fig. 2b reveals the corresponding coefficient of thermal expansion for the system DPPC/cholesterol as obtained from the PPC data. Notably, the $\alpha(T)$ curves exhibit a similar shape as the $C_p(T)$ data, an indication of the membrane enthalpy and volume fluctuations being govered by the same molecular origin. Below the main phase transition temperature of pure DPPC, $\alpha$ increases slightly with increasing temperature. Around the main phase transition temperature, $\alpha$ undergoes a rather sharp increase, reaches a maximum of about 0.15 K$^{-1}$ at $T_m$ (41.5 °C), and then rapidly decreases with increasing temperature, to reach a value close to that obtained below the transition temperature [$\alpha$ is $\sim 0.9 \cdot 10^{-3}$ K$^{-1}$ below the pretransition (20 °C) and $\sim 1.0 \cdot 10^{-3}$ K$^{-1}$ above the main transition (65 °C)]. The observed $\alpha$-value of pure DPPC is in the same range as that of other phospholipids [31, 33, 34, 37, 38], and similar to the thermal expansivity of pure liquid hydrocarbons, such as tetrade-

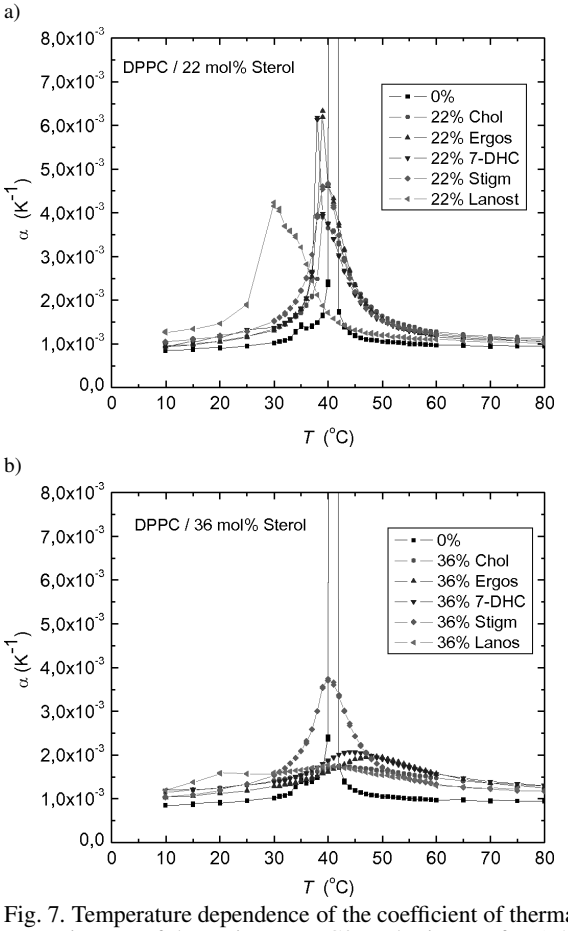


Fig. 7. Temperature dependence of the coefficient of thermal expansion, $\alpha$, of the various DPPC/sterol mixtures for a) 22 and b) 36 mol-% sterol.

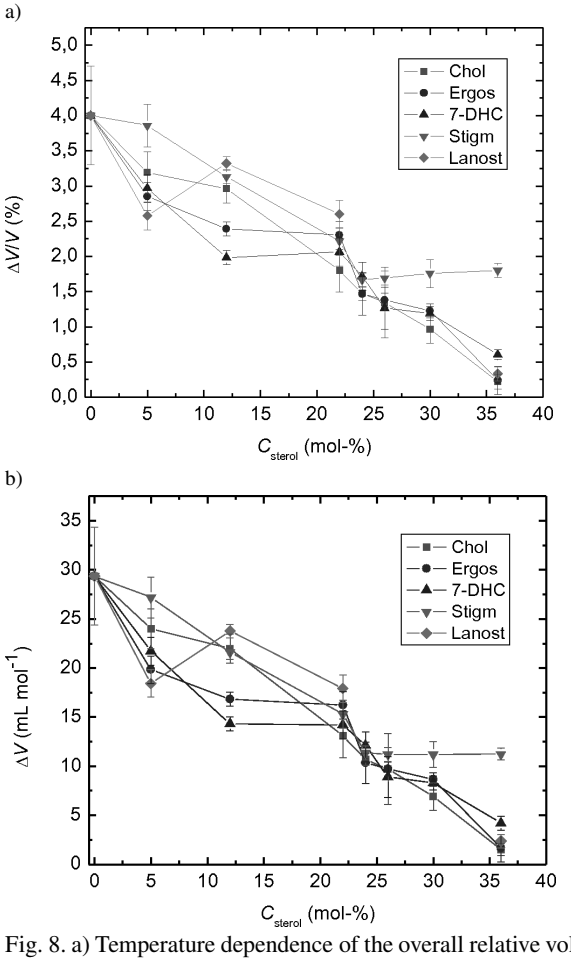


Fig. 8. a) Temperature dependence of the overall relative volume changes, $\Delta V/V$, and b) of the absolute volume change, $\Delta V$, of the various DPPC/sterol mixtures undergoing their chain-melting transitions.

cane ($\alpha$ = 0.9 $10^{-3}$ $K^{-1}$), but an order of magnitude larger than that of water [37].

With increasing cholesterol concentration, $\alpha$ increases slightly below and – notably, despite the condensing effect cholesterol imposes on fluid bilayers – also above $T_m$ (for example, $\alpha = 1.25 \cdot 10^{-3}$ $K^{-1}$ at 20 °C and $\alpha = 1.4 \cdot 10^{-3}$ $K^{-1}$ at 65 °C for 30 mol-% cholesterol in DPPC), whereas the main peak height of $\alpha$ in the transition region decreases and broadens markedly. Figs. 7a and 7b display the $\alpha(T)$-data in an expanded scale for all sterols at a concentration of 22 and 36 mol-%, respectively. Besides lanosterol, a qualitatively similar behavior of $\alpha(T)$ is observed for all sterols at a sterol concentration of 22 mol-% (Fig. 7a). The only significant differences are somewhat larger $\alpha$-values at the transition maxima. For the system DPPC/lanosterol, the asymmetric peak is broadened and shifted to a ~8 °C lower temperature, however, and the coefficient of thermal expansion is the largest one below $T_m$. Fig. 7b displays the corresponding PPC data for 36 mol-% sterol. As expected, the $\alpha$-values have further decreased in the phase transition region. For 7-DHC and ergosterol, the broad transition maxima have shifted to slightly higher temperatures if compared to cholesterol, whereas for lanosterol, again, a shift towards lower temperatures is observed. Notably, no such suppression of the transition is observed for DPPC/36 mol-% stigmasterol. The PPC data for both sterol concentrations indicate that cholesterol is most efficient in suppressing the chain-melting transition of the phospholipid bilayer system.

From an integration of the PPC data over the temperature range where the phase transitions occur, the

relative volume changes, $\Delta V/V$, of pure DPPC and the DPPC/sterol mixtures have also been determined (Fig. 8). While $\Delta V/V = 0.04 \pm 0.007$ (4 %), corresponding to an absolute volume change of 29 mL $mol^{-1}$, for pure DPPC, $\Delta V/V$ is $0.032 \pm 0.003$ for 5 mol-%, $0.03 \pm 0.002$ for 12 mol-%, and $0.013 \pm 0.005$ for 26 mol-% cholesterol, and continues to decrease with increasing sterol concentration, finally reaching $\Delta V/V = 0.002 \pm 0.001 \approx 0$ around 36 mol-% cholesterol. The corresponding width of the overall transition, $\Delta T_{1/2}$, increases from about 1 °C for the main transition of pure DPPC to about 13 °C for the DPPC/36 mol-% cholesterol mixture. The volume change associated with the pretransition of pure DPPC is a factor of about 10 smaller than that of the main transition.

Fig. 8 shows the relative volume changes, $\Delta V/V$, of pure DPPC and all DPPC/sterol mixtures as a function of the sterol concentration. Qualitatively, a similar, essentially linear behavior is observed for $\Delta V/V$ as a function of the sterol concentration for all DPPC/sterol mixtures. Only for the system DPPC/stigmasterol, a saturation behavior seems to occur above 24 mol-%. Notably, a similar behavior has been found for the order parameter profile of DPPC/stigmasterol as a function of sterol concentration [19].

## Concluding Remarks

The focus of this study was to identify and characterize the differential effects of various sterols, including cholesterol, the plant sterols ergosterol and stigmasterol, *trans*-7-dehydrocholesterol (7-DHC), and lanosterol, the evolutionary precursor of cholesterol, on the volumetric properties of the DPPC bilayer membrane and to relate these effects to the difference in their molecular chemistry (Fig. 1). To this end, PPC experiments have been carried out that allow determination of the temperature dependence of the expansion coefficient as well as volume changes accompanying lipid phase transitions.

Recent measurements of the lipid acyl-chain order parameter revealed that with increasing side-chain volume of the sterol, the conformational order of the lipid acyl-chains decreases, and an increase in alkyl chain volume has the most drastic effect on the condensing capacity of sterols [19]. The introduction of a double bond in the side chain counteracts this effect, owing to the decreased volume fluctuations in the steroid alkyl chain region. Introduction of a double bond in the ring system leads at low and medium-high sterol levels (up to ~40 mol-%) to a drastic increase in conformational order of the lipid acyl-chains (compare, *e. g*. *trans*-7-dehydrocholesterol with cholesterol), which can indeed be substantially higher than that induced by cholesterol. Additional methyl groups in the ring system of the sterol markedly counteract this rigidifying effect (compare lanosterol with ergosterol). Sterols with the bulkiest unsaturated side chains or sterol nuclei (stigmasterol, lanosterol) induce the smallest order-parameter increase of the fluid bilayer at high sterol concentrations (> 30 mol-%), and hence become less effective rigidifiers at high sterol levels. The difference might also be due to a different solubility/partitioning in the bilayer. Lanosterol is a sterol precursor. Owing to its additional methyl groups in the ring system, its partitioning is much less effective than that of cholesterol at high sterol levels. An important conclusion has been that cholesterol, with its streamlined molecular structure, interacts more effectively with lipid chains and stabilizes the liquid-ordered state. Interestingly, from an evolution point of view, cholesterol seems to be very efficient in suppressing the chain-melting transition of the phospholipid bilayer system. A marked limitation of the condensing effect is observed for the stigmasterol system having a rather bulky alkyl chain [19], which is also reflected in volumetric parameters as discussed above.

As shown here, alterations in the sterol structure are also reflected in their thermodynamic properties. Though the overall thermodynamic features of all sterols besides lanosterol seem to be qualitatively similar, minor differences are found, such as in abolishing the pretransition and in the extension of the phase space of the two-phase regions, as indicated by the differences observed in the corresponding DSC and PPC thermograms. For lanosterol, differences in the miscibility and temperature-concentration phase behavior and hence the thermodynamic functions $C_p(T)$ and $\alpha(T)$ are most obvious when compared to cholesterol and the other sterols.

Generally, the changes in $C_p(T)$ are found to precisely mirror the corresponding $\alpha(T)$ data, an indication that membrane enthalpy and volume fluctuations (Eqs. 3, 4) have the same molecular origin. Increases in $C_p(T)$ and $\alpha(T)$ at phase changes are mainly linked to cooperative fluctuations of large numbers of lipid molecules in their physical state [30, 46]. The sharpness of the transition peaks is related to the correlation lengths of these fluctuations, namely the domain

sizes of the coexisting phases. With increasing sterol concentration, the widths of both thermodynamic parameters at the chain-melting transitions increase drastically, indicating coupled enthalpy and volume fluctuations with low amplitude by large correlation lengths over an extended temperature region.

The large cross-sectional area of the steroid ring system of lanosterol makes this sterol a more effective spacer than DPPC molecules in the gel-state bilayer, thus relieving the mismatch in the cross-sectional areas of the acyl-chains and the DPPC polar headgroups at lower sterol concentrations more efficiently than cholesterol. Also, the rougher surface of the lanosterol molecule is expected to produce a greater amount of orientational disorder in the adjacent phospholipid's acyl-chains, thus further augmenting the expansion of the DPPC gel-state bilayer, and leading to the markedly larger $\alpha$-values observed for this system.

*Acknowledgement*

Financial support from the Deutsche Forschungsgemeinschaft, the state of Northrhine Westfalia and the European Union (Europäischer Fonds für regionale Entwicklung) is gratefully acknowledged.

[1] O. G. Mouritsen, M. J. Zuckermann, *Lipids* **2004**, *39*, 1101 – 1113.
[2] L. Finegold, *Cholesterol in Membrane Models*, CRC Press, Boca Raton, Florida **1993**.
[3] D. E. Vance, *Biochim. Biophys. Acta* **2000**, *1529*, 1 – 8.
[4] M. Bloom, O. G. Mouritsen, *Can. J. Chem.* **1988**, *66*, 706 – 712.
[5] R. A. Demel, B. de Kruyff, *Biochim. Biophys. Acta* **1976**, *457*, 109 – 132.
[6] P. L. Yeagle, *Biochim. Biophys. Acta* **1985**, *822*, 267 – 287.
[7] M. J. Zuckermann, J. H. Ipsen, L. Miao, O. G. Mouritsen, M. Nielsen, J. Polson, J. Thewalt, I. Vattulainen, H. Zhu, *Methods in Enzymology* **2004**, *383*, 198 – 229.
[8] J. B. Finean, *Chem. Phys. Lipids* **1990**, *54*, 147 – 156.
[9] H. Yamauchi, Y. Takao, M. Abe, K. Ogino, *Langmuir* **1993**, *9*, 300 – 304.
[10] T. P. W. McMullen, R. N. A. H. Lewis, R. N. McElhaney, *Biophys. J.* **1994**, *66*, 741 – 752.
[11] J. P. Slotte, M. Jungner, C. Vilchèze, R. Bittman, *Biochim. Biophys. Acta* **1994**, *1190*, 435 – 443.
[12] J. P. Slotte, *Biochim. Biophys. Acta* **1995**, *1237*, 127 – 134.
[13] C. Bernsdorff, R. Winter, *Ber. Bunsen-Ges. Phys. Chem.* **1995**, *99*, 1479 – 1487.
[14] C. Bernsdorff, R. Winter, *Z. Phys. Chem.* **1996**, *193*, 151 – 173.
[15] C. Bernsdorff, R. Winter, *Biophys. J.* **1997**, *71*, 1264 – 1277.
[16] O. Reis, R. Winter, T. W. Zerda, *Biochim. Biophys. Acta* **1996**, *1279*, 5 – 16.
[17] E. Endress, S. Bayerl, K. Prechtel, C. Maier, R. Merkel, T. M. Bayerl, *Langmuir* **2002**, *18*, 3293 – 3299.
[18] L. Miao, M. Nielsen, J. Thewalt, J. H. Ipsen, M. Bloom, M. J. Zuckermann, O. G. Mouritsen, *Biophys. J.* **2002**, *82*, 1429 – 1444.
[19] C. Bernsdorff, R. Winter, *J. Phys. Chem. B* **2003**, *107*, 10658 – 10664.
[20] J. H. Ipsen, G. Karlström, O. G. Mouritsen, H. Wennerström, M. J. Zuckermann, *Biochim. Biophys. Acta* **1987**, *905*, 162 – 172.
[21] J. Ipsen, O. G. Mouritsen, M. Bloom, *Biophys. J.* **1990**, *57*, 405 – 412.
[22] M. R. Vist, J. H. Davis, *Biochemistry* **1990**, *29*, 451 – 464.
[23] Y.-W. Hsueh, K. Gilbert, C. Trandum, M. Zuckermann, J. Thewalt, *Biophys. J.* **2005**, *88*, 1799 – 1808.
[24] M. B. Sankaram, T. E. Thompson, *Proc. Natl. Acad. Sci. USA* **1991**, *88*, 8686 – 8690.
[25] Y.-W. Chiang, A. J. Costa-Filho, J. H. Freed, *J. Phys. Chem. B* **2007**, *111*, 11260 – 11270.
[26] R. Wu, L. Chen, Z. Yu, P. J. Quinn, *Biochim. Biophys. Acta* **2006**, *1758*, 764 – 771.
[27] T. P. W. McMullen, R. N. McElhaney, *Biochim. Biophys. Acta* **1995**, *1234*, 90 – 98.
[28] T. P. W. McMullen, R. N. A. H. Lewis, R. N. McElhaney, *Biochemistry* **1993**, *32*, 516 – 522.
[29] D. A. Mannock, R. N. A. H. Lewis, R. N. McElhaney, *Biophys. J.* **2006**, *91*, 3327 – 3340.
[30] R. Krivanek, L. Okoro, R. Winter, *Biophys. J.*, in press.
[31] M. Böttner, R. Winter, *Biophys. J.* **1993**, *65*, 2041 – 2046.
[32] H. Seemann, R. Winter, *Z. Phys. Chem.* **2003**, *217*, 831 – 846.
[33] D. L. Melchior, F. J. Scavitto, J. M. Steim, *Biochemistry* **1980**, *19*, 4828 – 4834.
[34] J. F. Nagle, D. A. Wilkinson, *Biophys. J.* **1978**, *23*, 159 – 175.
[35] G. Cevc, D. Marsh, *Phospholipid Bilayers*, John Wiley & Sons, New York **1987**.
[36] M. Edidin, *Ann. Rev. Biophys. Biomol. Struct.* **2003**, *32*, 257 – 283.
[37] H. Heerklotz, J. Seelig, *Biophys. J.* **2002**, *82*, 1445 – 1452.
[38] H. Heerklotz, A. Tsamaloukas, *Biophys. J.* **2006**, *91*, 600 – 607.

[39] R. Ravindra, R. Winter, *ChemPhysChem* **2003**, *4*, 359 – 365.
[40] W. Dzwolak, R. Ravindra, J. Lendermann, R. Winter, *Biochemistry* **2003**, *42*, 11347 – 11355.
[41] R. Ravindra, C. Royer, R. Winter, *Phys. Chem. Chem. Phys*. **2004**, *6*, 1952 – 1961.
[42] R. Ravindra, R. Winter, *ChemPhysChem* **2004**, *5*, 566 – 571.
[43] L. Mitra, N. Smolin, R. Ravindra, C. Royer, R.Winter, *Phys. Chem. Chem. Phys*. **2006**, *8*, 1249 – 1265.
[44] A. I. Greenwood, S. Tristram-Nagle, J. F. Nagle, *Chem. Phys. Lipids* **2006**, *143*, 1 – 10.
[45] V. Smirnovas, R. Winter, T. Funck, W. Dzwolak, *ChemPhysChem* **2006**, *7*, 1046 – 1049.
[46] H. Ebel, P. Grabitz, T. Heimburg, *J. Phys. Chem*. **2001**, *105*, 7353 – 7360.